An interaction-driven quantum many-body engine enabled by atom-atom correlations

R. S. Watson and K. V. Kheruntsyan
School of Mathematics and Physics, University of Queensland, Brisbane, Queensland 4072, Australia
(Dated: August 11, 2023)

Quantum heat engines are capable of utilizing uniquely quantum many-body effects to enhance the performance of classical engine cycles, implying a quantum advantage. Here we propose and investigate the performance of a quantum many-body Otto cycle operating under a sudden interaction quench protocol, with a one-dimensional (1D) Bose gas as a working fluid. We show that the very operation of this Otto cycle as an engine is enabled by atom-atom correlations in the system. These correlations are different from those in a classical ideal gas, and are a result of the interplay between quantum statistics, interparticle interactions, and thermal fluctuations; extracting positive net work from the system without such correlations would be impossible. We also demonstrate how the performance of the engine can be further enhanced by allowing particle exchange between the system and the thermal reservoirs, in addition to heat exchange. We evaluate the performance of the engine using approximate analytic and exact thermodynamic Bethe ansatz results available for the Lieb-Liniger model that describes the 1D Bose gas, but we emphasise that the broad conclusions arrived at here are not limited to this particular model.

Introduction.—Quantum heat engines (QHE's) are central in the theoretical and experimental development of quantum thermodynamics—an emerging field devoted to the exploration of thermodynamical processes in a quantum mechanical context [1–11]. These engines, which can be traced back to 1959 [12], play a similar role in the development of quantum thermodynamics that their macroscopic counterparts played in fuelling scientific advancement during the Industrial Revolution [13–15]. In the past decade, advances in the control over quantum platforms, such as single ions [16–18], nitrogen vacancy centers [19], and single-atom impurities immersed in an ultra-cold atomic bath [20], have led to the realization of single-particle QHE's, representing the limit in the creation of an 'infinitesimal machine' [21].

However, in order to utilize the breadth of quantum resources available, one must move beyond single-particle systems to engines that utilize many-body interactions. Such QHE's are uniquely positioned to take advantage of quantum resources, such as entanglement [22–25], correlations [26–28], or quantum coherence [29–34], to enhance performance. Many-body QHE's have been shown to be capable of outperforming an ensemble of single-particle engines operating with the same resources [35]. Control over inter-particle interactions, in particular, allows for the creation of uniquely many-body QHE's [36–40], which have recently been realized in the laboratory [41, 42]. Such rapid experimental development underscores the need for further theoretical studies of thermodynamical processes in the context of quantum many-body interacting systems.

In this Letter, we propose a quantum many-body Otto engine using a finite temperature one-dimensional (1D) Bose gas with contact interactions as the working fluid, in which the unitary work strokes are driven by a sudden quench of the interaction strength. The benefits of using the 1D Bose gas is that the underlying theoretical model—the Lieb-Liniger model—is exactly solvable in the uniform limit [43–45], in addition to being experimentally realizable using ultracold atomic gases confined to highly anisotropic traps [46–72]. This offers unique opportunities for gaining physical insights into the performance of such an engine as a tractable and testable quantum many-body problem. The 1D Bose gas has a rich equilibrium phase diagram [73, 74] which spans several nontrivial regimes, from the weakly interacting quasicondensate through to the strongly interacting Tonks-Girardeau regime of fermionization [56, 73–82]. We demonstrate how the thermodynamic performance, in particular net work and efficiency, of this many-body QHE can be calculated through the experimentally measurable atom-atom pair correlation [57, 73, 74], internal energy, and density profile of an ultracold quantum gas.

Interaction-driven Otto cycle.—In 1D Bose gases confined to highly anisotropic harmonic traps with longitudinal and transverse frequencies ω and $\omega_\perp$ such that $\omega \ll \omega_\perp$, the 1D interaction strength can be expressed as $g \simeq 2\hbar\omega_\perp a_s$, away from confinement induced resonances [83], where a_s is the 3D s-wave scattering length. Changing the interaction strength g may be achieved by tuning the magnetic field that controls the transverse confinement frequency $\omega_\perp$, which leads to a volume change of the gas (i.e., transverse expansion or compression), and hence can be thought of as analogous to mechanical work in the conventional Otto cycle [84] (see also [85]).

The interaction-driven Otto engine cycle consists of four strokes (see Fig. 1): (1) *Unitary expansion,* $\mathbf{A}\to\mathbf{B}$: the working fluid, consisting of N total atoms at interaction strength g_h, initially in a thermal equilibrium state at temperature T_h of the hot reservoir, is decoupled from the reservoir and has its interaction strength quenched to $g_c < g_h$, generating beneficial work out $W_{\rm out} = \langle \hat{H}\rangle_{\mathbf{A}} - \langle \hat{H}\rangle_{\mathbf{B}} > 0$ done by the fluid, where $\hat{H}$ is the system Hamiltonian [86], and $\langle \hat{H}\rangle_{\mathbf{i}}$ is its expec-

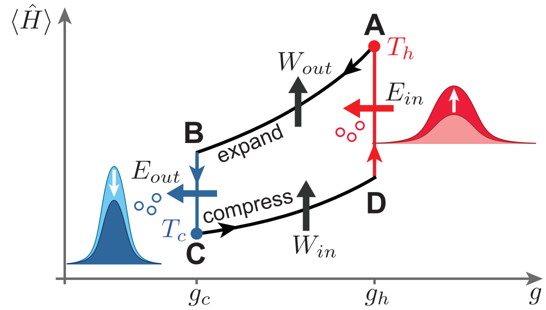

FIG. 1. An interaction-driven quantum many-body Otto cycle, operating between two interaction strengths, g_c and g_h. Unitary strokes (**AB** and **CD**) are shown in black, while non-unitary thermalization strokes (**BC** and **DA**) are color-coded to the cold (blue) and hot (red) reservoirs at temperatures T_c and T_h, respectively. In addition to the regular Otto cycle, which does not involve any exchange of particles between the system and reservoirs, we also show a modified version of the cycle, in which such exchange is allowed; the latter is illustrated via the cartoons of the system density profiles that either grow or decrease, depending on whether particles flow in from the hot reservoir or out into the cold reservoir.

tation value for the total energy of the system in state $\mathbf{i} = \{\mathbf{A,B,C,D}\}$. (2) *Thermalization with cold reservoir*, $\mathbf{B}\to\mathbf{C}$: the working fluid is connected to a thermal reservoir at temperature T_c and allowed to equilibrate at constant interaction strength g_c, transferring energy in the form of heat $Q_{\rm out} = \langle \hat{H} \rangle_{\mathbf{B}} - \langle \hat{H} \rangle_{\mathbf{C}} > 0$ to the cold reservoir where $Q_{\rm out(in)} \equiv E_{\rm out(in)}$ for a purely thermal system-reservoir contact in Fig. 1. (3) *Unitary compression*, $\mathbf{C}\to\mathbf{D}$: disconnected from the cold reservoir, the working fluid has its interaction strength quenched from $g_c \to g_h$, with work $W_{\rm in} = \langle \hat{H} \rangle_{\mathbf{D}} - \langle \hat{H} \rangle_{\mathbf{C}} > 0$ done on the fluid. (4) *Thermalization with hot reservoir*, $\mathbf{D}\to\mathbf{A}$: the working fluid is connected to a reservoir at temperature T_h, where it is left to equilibrate, taking in heat $Q_{\rm in} = \langle \hat{H} \rangle_{\mathbf{A}} - \langle \hat{H} \rangle_{\mathbf{D}} > 0$ from the hot reservoir, returning to the initial thermal state of the overall cycle. Such an engine cycle generates net positive work $W = W_{\rm out} - W_{\rm in} > 0$, if $\langle \hat{H} \rangle_{\mathbf{A}} - \langle \hat{H} \rangle_{\mathbf{D}} > \langle \hat{H} \rangle_{\mathbf{B}} - \langle \hat{H} \rangle_{\mathbf{C}}$, with efficiency $\eta = W/Q_{\rm in} = 1 - Q_{\rm out}/Q_{\rm in}$ [14, 15].

In this work, we specifically consider a sudden or instantaneous quench of the interaction strength g in the unitary strokes of the Otto cycle. Realistically, such a sudden quench from $g_{c(h)}$ to $g_{h(c)}$ would still occur over a finite duration Δt, and the "instantaneity" of the quench here refers to the assumption that Δt is much shorter than the characteristic time of longitudinal dynamics, i.e. that $\Delta t \ll 2\pi/\omega$. Thus, it is with respect to the *longitudinal* dynamics that we refer to our quench as sudden. With respect to the *transverse* dynamics, on the other hand, we are assuming that Δt is sufficiently long compared to the characteristic transverse timescale, $2\pi/\omega_\perp \ll \Delta t$. In this case, the quench would retain the system in the transverse ground state, hence without compromising the 1D character of the system. As such, the work done on (or by) the system during the unitary strokes can be regarded as transversely quasi-static.

Under such a sudden quench, all expectation values over field operators in the system Hamiltonian before (i) and after (f) the quench remain unchanged. Hence, the only contribution to the difference in total energy between pre- and post-quench states, $\langle \hat{H} \rangle_f - \langle \hat{H} \rangle_i$, comes from the difference between the interaction terms, $\frac{1}{2} g_f \int dz \langle \hat{\Psi}^\dagger \hat{\Psi}^\dagger \hat{\Psi} \hat{\Psi} \rangle_f - \frac{1}{2} g_i \int dz \langle \hat{\Psi}^\dagger \hat{\Psi}^\dagger \hat{\Psi} \hat{\Psi} \rangle_i$, where $\langle \hat{\Psi}^\dagger \hat{\Psi}^\dagger \hat{\Psi} \hat{\Psi} \rangle_f = \langle \hat{\Psi}^\dagger \hat{\Psi}^\dagger \hat{\Psi} \hat{\Psi} \rangle_i$ in a sudden quench, and $\hat{\Psi}^\dagger(z)$ and $\hat{\Psi}(z)$ represent the field creation and annihilation operators. Accordingly, the energy difference can be expressed as $\langle \hat{H} \rangle_f - \langle \hat{H} \rangle_i = \frac{1}{2}(g_f - g_i) \overline{G_i^{(2)}}$, where we have defined the total (integrated) correlation of the thermal equilibrium state $\overline{G_i^{(2)}} = \int dz \langle \hat{\Psi}^\dagger \hat{\Psi}^\dagger \hat{\Psi} \hat{\Psi} \rangle_i$ [74].

Identifying the i and f states as **A** (h) and **B**, or as **C** (c) and **D**, the net work can be expressed as

$$W = \frac{1}{2}(g_h - g_c) \left(\overline{G_h^{(2)}} - \overline{G_c^{(2)}} \right), \qquad (1)$$

where states h and c are thermal equilibrium states of the gas in contact with hot and cold reservoirs. Likewise, the efficiency may be expressed as,

$$\eta = 1 - \frac{\langle \hat{H} \rangle_h - \langle \hat{H} \rangle_c - \frac{1}{2}(g_h - g_c) \overline{G_h^{(2)}}}{\langle \hat{H} \rangle_h - \langle \hat{H} \rangle_c - \frac{1}{2}(g_h - g_c) \overline{G_c^{(2)}}}. \qquad (2)$$

These equations allow for investigation of the interaction-driven quantum Otto cycle under a sudden quench protocol through solely the equilibrium properties of the gas.

Though we began our discussion having in mind a harmonically trapped 1D Bose gas as a working fluid, our results so far are general enough to be applicable in arbitrary longitudinal confinement. In particular, this includes a uniform 1D Bose gas on a ring, which is the prototypical model originally introduced by Lieb and Liniger [43]. Because of this, and for analytical insight, we proceed by first presenting results for a uniform system [87], before considering the harmonically trapped case.

Uniform gas as a working fluid.—Finite-temperature uniform 1D Bose gases have no phase transition to a true Bose-Einstein condensate in the thermodynamic limit, unlike Bose-Einstein condensation in three dimensions [88, 89]. However, there still exists a rich crossover phase diagram of different regimes [73, 74], that can be parameterized by dimensionless interaction strength, $\gamma = mg/\hbar^2\rho$, and temperature, $\tau = 2mk_BT/\hbar^2\rho^2$, where m is the bosonic mass and $\rho = N/L$ is the 1D density for N atoms in a system of length L.

For a uniform 1D Bose gas, the total correlation in the hot (h) or cold (c) thermal equilibrium state may be expressed as $\overline{G^{(2)}_{h(c)}} = N\rho g^{(2)}_{h(c)}(0)$ [86], where $g^{(2)}_{h(c)}(0)$ is the normalized local (same point) atom-atom correlation function [73]. Combining this with Eq. (1), the net work per particle can be expressed as

$$\frac{W}{N} = \frac{\hbar^2\rho^2}{2m}(\gamma_h - \gamma_c)\left(g^{(2)}_h(0) - g^{(2)}_c(0)\right). \qquad (3)$$

From this equation, and given that γ_h is always larger than γ_c, we note that if the local pair correlations did not depend on the respective interaction strengths and temperatures, i.e. if they were the same, $g^{(2)}_h(0) = g^{(2)}_c(0)$, then the net work per particle would vanish. This implies that such an Otto cycle would never operate as an engine that converts heat into net positive work. We therefore conclude that extracting positive net work, $W/N > 0$, from this Otto cycle can only be enabled by atom-atom correlations. More specifically, the only way to extract positive net work is to have $g^{(2)}_h(0)/g^{(2)}_c(0) > 1$.

Net work and efficiency of the quantum Otto cycle with a working fluid consisting of a uniform gas, calculated using analytic approximations to the atom-atom correlation function for the weakly interacting 1D Bose gas in a quasicondensate regime (see Appendix A and Ref. [73]) realizable in typical experiments are shown in Fig. 2 (a) and (b) as a function of the ratio of temperatures, T_h/T_c, and interaction strengths, g_h/g_c, of the thermal equilibrium states. The cold thermal state **C** of the cycle is defined by $\gamma_c = 5\times10^{-3}$ and $\tau_c = 1.3\times10^{-2}$. The observed increase of net work under large temperature ratios may be attributed to the linear dependence of Eq. (3) on the local correlation of the hot thermal state $g^{(2)}_h(0) \simeq 1 + \frac{1}{2}\tau_h\gamma_h^{-1/2}$, for $\gamma_h \ll \tau_h \ll \sqrt{\gamma_h}$ [73]. On the other hand, the unfavorable inverse dependence of the correlation function on the square root of the interaction strength results in no positive net work under large interaction strength ratios.

Harmonically trapped working fluid.—For a harmonically trapped 1D Bose gas, the total correlation of the thermal equilibrium states can be approximated as $\overline{G^{(2)}_{h(c)}} \simeq N_{h(c)} b_{h(c)} \rho_{h(c)}(0) g^{(2)}_{h(c)}(0,0)$ [86], where $N_{h(c)}$ is the total atom number of the system in the hot (cold) thermal equilibrium state (where we will consider the possibility of $N_h \neq N_c$ in the next section below), $g^{(2)}_{h(c)}(0,0)$ is the normalized local atom-atom correlation function in the trap center $z = 0$ [74], and $b_{h(c)}$ is a dimensionless factor of order one that depends on the shape of the density profile [86]. Combining this with Eq. (1), the net work per particle may be approximated as

$$W \simeq \frac{g_h - g_c}{2}\left(b_h g^{(2)}_h(0,0)\rho_h(0)N_h - b_c g^{(2)}_c(0,0)\rho_c(0)N_c\right). \qquad (4)$$

Eqs. (3) and (4) represent the main results of this letter.

We see from Eq. (4) that, if $g^{(2)}_h(0,0) = g^{(2)}_c(0,0) \equiv g^{(2)}(0,0)$, then net work per particle would simplify to $W/N \simeq \frac{1}{2}b(g_h - g_c)g^{(2)}(0,0)\left(\rho_h(0) - \rho_c(0)\right)$ and would never be positive, where we have taken $N_h = N_c \equiv N$ and have also assumed that the geometric factors b_h and b_c are approximately the same ($b_h \simeq b_c = b$) for small quenches. This is true because $g_h > g_c$ by definition and because the peak densities normally satisfy $\rho_h(0) < \rho_c(0)$ (as the peak density is typically monotonically decreasing with both the interaction strength and temperature). In order to gain positive net work from such an engine, one has to still have $g^{(2)}_h(0,0)/g^{(2)}_c(0,0) > 1$, but this condition is no longer sufficient, unlike the previous case of a uniform system. Instead, one must satisfy a more demanding condition $g^{(2)}_h(0,0)/g^{(2)}_c(0,0) > \rho_c(0)/\rho_h(0) > 1$ (for $b_h = b_c$), which reduces the parameter space over which the net work is positive. In a calculation beyond the approximations of Eq. (4), all these conclusions are implicitly embedded in the original exact expression for the net work Eq. (1), expressed in terms of the average correlation $\overline{G^{(2)}_{h(c)}}$, which can be evaluated numerically using the Yang-Yang thermodynamic Bethe ansatz (TBA) and the local density approximations (LDA) (see Appendix A and Refs [73, 74]).

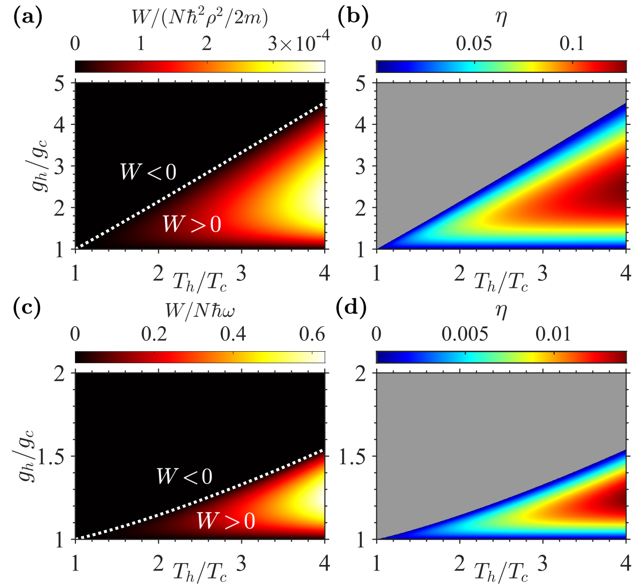

FIG. 2. Net work and efficiency of an interaction-quench Otto engine with a 1D quasicondensate working fluid. The net work, W, and efficiency, η, of the engine, for a uniform system of 1D density ρ, are shown in panels (a) and (b), respectively, as functions of the ratio of reservoir temperatures, T_h/T_c, and interaction strengths, g_h/g_c, of the hot (h) and cold (c) thermal equilibrium states. Here, the cold equilibrium state is defined through the dimensionless interaction strength $\gamma_c = 5\times10^{-3}$ and dimensionless temperature $\tau_c = 1.3\times10^{-2}$ [90]. Panels (c) and (d) show the same, but for a harmonically trapped quasicodensate, with a total of $N = 2000$ particles. The cold equilibrium state has an interaction strength and temperature of $\overline{g}_c = 0.6$ and $\overline{T}_c = 100$, respectively [91].

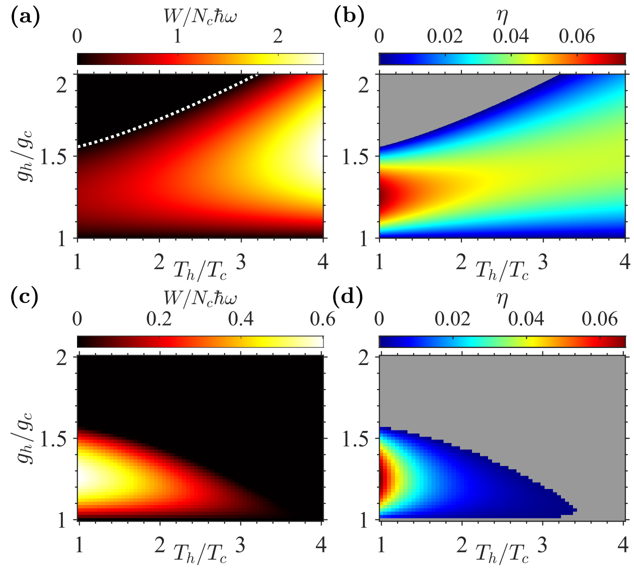

FIG. 3. Net work and efficiency of the same harmonically trapped system shown in Fig. 2 (c) and (d) but here under a finite particle flow from the hot to the cold reservoir of $\Delta N = 200$ (with $N_h = N_c + \Delta N = 2200$), where net work is normalized to $N_c = 2000$. Panels (a) and (b) show analytic approximation of the engine performance, whereas in panels (c) and (d), we demonstrate the exact numeric evaluation of performance via the Yang-Yang TBA.

Net work and efficiency of a harmonically trapped 1D Bose gas in a weakly interacting quasicondensate regime are shown in Fig. 2 (c) and (d), where we used the Thomas-Fermi approximation for the density profile, in combination with analytic approximations for the atom-atom correlation function (see Appendix A). Here, the working fluid contains $N = 2000$ atoms, with the cold thermal state **C** of the cycle defined by an interaction strength, $\overline{g}_c = 0.6$, and temperature $\overline{T}_c = 100$, here written in natural units of the longitudinal harmonic oscillator frequency ω [91]. We observe a similar behaviour as seen in the uniform gas for large temperature and interaction strength ratios. However, for the harmonically trapped gas, the total correlation, $\overline{G_h^{(2)}}$, is directly dependent on the central density which scales as $\overline{\rho}_h(0) \propto \overline{g}_h^{-1/3}$ (in the quasicondensate regime under consideration), resulting in a decreased range of the interaction strength ratio over which the engine operates with $W/N > 0$.

Performance boost under particle exchange.—We now demonstrate how the performance of the interaction-driven Otto cycle can be further increased by allowing for a particle exchange $\pm\Delta N$ between the system and the hot and cold reservoirs, i.e. the case where $N_h \neq N_c$ in Eq. (4). Given the number of particles in the system, N_c, in the cold thermal equilibrium state **C** and in the unitary compression stroke **C**→**D**, we now allow for a flow of ΔN particles from the hot reservoir to the system in the thermalization stage **D**→**A** (see Fig. 1) [92]. This means that the hot thermal equilibrium state **A** and the unitary expansion stroke **A**→**B** now has $N_h = N_c + \Delta N$ particles. We further assume that the excess of particles, ΔN, is then dumped into the cold reservoir during the thermalization stage **B**→**C**, so that the system returns to having the original number of particles N_c for the cycle to repeat. We immediately see in Eq. (4) that $N_h > N_c$ acts as an additional factor that may compensate for the unfavorable relation of $\rho_h(0) < \rho_c(0)$, that we already discussed in the $N_h = N_c = N$ case, and hence can increase the engine performance.

Performance of the quantum Otto cycle under a finite particle exchange of $\Delta N = 200$ is demonstrated in Fig. 3, where the cold equilibrium state is the same as that in Figs. 2 (c) and (d). Analytic evaluation of the net work and efficiency is shown in panels (a) and (b), respectively. We observe here an increase in both maximum net work and the range of parameters over which the net work is positive due to the dependence of Eq. (4) on N_h. Utilizing next Eq. (1), in combination with the LDA and the numerically exact Yang-Yang TBA, we evaluate the performance of this cycle without approximation, results of which are shown in Fig. 3 (c) and (d). Disagreement between the approximate analytic and TBA results under increasing temperature ratio arises here due to the limits on the applicability of the analytic approximations used in Eq. (4) (see Appendix B). However, the agreement between analytic and TBA results is excellent around $T_h/T_c = 1$ [86], where we note that the quantum Otto cycle for this ratio of temperatures corresponds to the finite temperature extension and sudden quench limit of the 'Feshbach engine' cycle investigated in Ref. [39].

Summary.—We have proposed a sudden interaction-quench Otto cycle operating in a quantum many-body system using a 1D Bose gas as a working fluid. Extracting positive net work from such an engine was shown to be enabled by atom-atom correlations that generally have nontrivial dependence on the interparticle interaction strength and temperature of the system. Additional particle exchange between the system and the reservoirs during the thermalization strokes was shown to further enhance the engine performance. Both these effects counter the unfavorable temperature dependence of the peak density of the harmonically trapped gas that can hinder the extraction of positive net work from the engine. Outside the applicable regimes of analytic approximations involved in Eqs. (4)–(5), we have evaluated the engine performance using the Yang-Yang thermodynamic Bethe ansatz, for experimentally realistic parameters. Even though our specific results for the net work and the efficiency were calculated for a 1D Bose as an example, the broad conclusions arrived at here on the basis of equations (1)–(4) are applicable to other related systems, such as ultra-cold 2D and 3D Bose gases, and should aid the tests and realization of quantum thermodynamic concepts in laboratory settings.

This work was supported through Australian Research Council Discovery Project Grant No. DP190101515.

Appendix A: Interaction-driven Otto cycle in a quasicondensate regime.—In the weakly interacting thermal quasicondensate regime of the 1D Bose gas, dominated by thermal (rather than quantum) fluctuations, and corresponding to $\gamma \ll \tau \ll \sqrt{\gamma}$ [73], the normalized local two-body correlation function may be approximated for a uniform gas as [73, 74, 93]:

$$g^{(2)}(0) \simeq 1 + \frac{1}{2}\frac{\tau}{\sqrt{\gamma}} + \frac{\zeta(1/2)}{\sqrt{\pi}}\sqrt{\tau} - \frac{2\zeta(-1/2)}{\sqrt{\pi}}\frac{\gamma}{\sqrt{\tau}}, \quad (5)$$

where $\zeta(s)$ is the Riemann zeta function of $s \in \mathbb{R}$. This is the expression that was used in combination with Eq. (3) to generate the example of W/N in Fig. 2 (a). For evaluating the engine efficiency, we additionally used an approximate analytic expression for the total internal energy of the gas, given in this regime by [93]:

$$\langle \hat{H} \rangle = N\frac{\hbar^2\rho^2}{2m}\bigg(\gamma + \frac{\zeta(3/2)}{4\sqrt{\pi}}\tau^{3/2} + \frac{\zeta(1/2)}{2\sqrt{\pi}}\tau^{1/2}\gamma - \frac{3\zeta(-1/2)}{2\sqrt{\pi}}\tau^{-1/2}\gamma^2\bigg). \quad (6)$$

For a harmonically trapped gas in the same thermal quasicondensate regime the density profile is well approximated by the Thomas-Fermi (TF) parabola, $\rho(z) = \rho(0)\left(1 - z^2/R^2\right)$, for $|z| < R$, and $\rho(z) = 0$ otherwise, where $\rho(0) = \left(9mN^2\omega^2/32g\right)^{1/3}$ is the peak density and $R = \left(3Ng/2m\omega^2\right)^{1/3}$ is the TF radius [88, 89]. From this, we derive the constant dimensionless factor $b_h \simeq b_c = b = 4/5$ in Eq. (4) [86]. The TF density profile, along with Eq. (5), where γ and τ are replaced by their values at the trap center [74], may then be combined with Eqs. (2) and (4), producing analytic expressions for the net work and efficiency of the cycle. This prescription was used to produce Figs. 2 (c)-(d), and Figs. 3 (a)-(b).

Appendix B: Experimental considerations.—Experimental realization of a harmonically trapped 1D Bose gas often falls outside the asymptotic regimes where analytic approximations such as Eq. (5) are applicable. In such situations, we may utilize the exact Yang-Yang TBA [44, 45], in combination with the LDA [74, 86], to evaluate the equilibrium properties of the gas required for calculating W and η via Eqs. (1) and (2). This approach is utilized in Figs. 3(c) and (d). Here, large net work is obtained under a small temperature ratio, as a small difference in temperature will ensure that the peak density is not greatly reduced due to the increased population in the thermal tails. The difference between the cycle performance based on analytics, shown in Figs. 3(a)-(b), and that based on numerics, shown in Figs. 3(c)-(d), is due to the crudeness of approximations used in Eq. (4) (as opposed to the exact Eq. (1)) for the cycle parameters, which neglected the dependence of the peak density on the temperature due to the assumed Thomas-Fermi approximation.

[1] R. Kosloff and A. Levy, Quantum Heat Engines and Refrigerators: Continuous Devices, Annual Review of Physical Chemistry **65**, 365 (2014).
[2] R. Kosloff, Quantum thermodynamics: A dynamical viewpoint, Entropy **15**, 2100 (2013).
[3] S. Vinjanampathy and J. Anders, Quantum thermodynamics, Contemporary Physics **57**, 545 (2016).
[4] J. Millen and A. Xuereb, Perspective on quantum thermodynamics, New Journal of Physics **18**, 011002 (2016).
[5] J. Anders and M. Esposito, Focus on quantum thermodynamics, New J. Phys **19**, 010201 (2017).
[6] R. Alicki and R. Kosloff, Introduction to quantum thermodynamics: History and prospects, in *Thermodynamics in the Quantum Regime: Fundamental Aspects and New Directions*, edited by F. Binder, L. A. Correa, C. Gogolin, J. Anders, and G. Adesso (Springer International Publishing, Cham, 2018) pp. 1–33.
[7] S. Deffner and S. Campbell, *Quantum Thermodynamics: An introduction to the thermodynamics of quantum information* (Morgan & Claypool Publishers, San Rafael, 2019).
[8] T. Fogarty and T. Busch, A many-body heat engine at criticality, Quantum Science and Technology **6**, 015003 (2020).
[9] A. Hartmann, V. Mukherjee, W. Niedenzu, and W. Lechner, Many-body quantum heat engines with shortcuts to adiabaticity, Physical Review Research **2**, 023145 (2020).
[10] V. Mukherjee and U. Divakaran, Many-body quantum thermal machines, Journal of Physics: Condensed Matter **33**, 454001 (2021).
[11] M. Gluza, J. a. Sabino, N. H. Ng, G. Vitagliano, M. Pezzutto, Y. Omar, I. Mazets, M. Huber, J. Schmiedmayer, and J. Eisert, Quantum Field Thermal Machines, PRX Quantum **2**, 030310 (2021).
[12] H. E. D. Scovil and E. O. Schulz-DuBois, Three-Level Masers as Heat Engines, Phys. Rev. Lett. **2**, 262 (1959).
[13] S. Carnot, *Reflections on the motive power of heat and on machines fitted to develop that power* (J. Wiley, Hoboken, New Jersey, 1890).
[14] D. V. Schroeder, *An introduction to thermal physics* (Oxford University Press, Oxford, 2020).
[15] H. B. Callen, *Thermodynamics and an introduction to thermostatistics*, 2nd ed. (John Wiley & Sons, Hoboken, New Jersey, 1985).
[16] J. Roßnagel, S. T. Dawkins, K. N. Tolazzi, O. Abah, E. Lutz, F. Schmidt-Kaler, and K. Singer, A single-atom heat engine, Science **352**, 325 (2016).
[17] D. von Lindenfels, O. Gräb, C. T. Schmiegelow, V. Kaushal, J. Schulz, M. T. Mitchison, J. Goold, F. Schmidt-Kaler, and U. G. Poschinger, Spin Heat Engine Coupled to a Harmonic-Oscillator Flywheel, Phys. Rev. Lett. **123**, 080602 (2019).
[18] N. Van Horne, D. Yum, T. Dutta, P. Hänggi, J. Gong, D. Poletti, and M. Mukherjee, Single-atom energy-

conversion device with a quantum load, npj Quantum Information **6**, 37 (2020).

[19] J. Klatzow, J. N. Becker, P. M. Ledingham, C. Weinzetl, K. T. Kaczmarek, D. J. Saunders, J. Nunn, I. A. Walmsley, R. Uzdin, and E. Poem, Experimental Demonstration of Quantum Effects in the Operation of Microscopic Heat Engines, Phys. Rev. Lett. **122**, 110601 (2019).

[20] Q. Bouton, J. Nettersheim, S. Burgardt, D. Adam, E. Lutz, and A. Widera, A quantum heat engine driven by atomic collisions, Nature Communications **12**, 2063 (2021).

[21] R. Feynman, There's plenty of room at the bottom, in *Feynman and computation* (CRC Press, Boca Raton, Florida, United States, 2018) pp. 63–76.

[22] F. G. Brandao and M. B. Plenio, Entanglement theory and the second law of thermodynamics, Nature Physics **4**, 873 (2008).

[23] S. Hilt and E. Lutz, System-bath entanglement in quantum thermodynamics, Phys. Rev. A **79**, 010101 (2009).

[24] K. Funo, Y. Watanabe, and M. Ueda, Thermodynamic work gain from entanglement, Phys. Rev. A **88**, 052319 (2013).

[25] R. Alicki and M. Fannes, Entanglement boost for extractable work from ensembles of quantum batteries, Phys. Rev. E **87**, 042123 (2013).

[26] J. Oppenheim, M. Horodecki, P. Horodecki, and R. Horodecki, Thermodynamical Approach to Quantifying Quantum Correlations, Phys. Rev. Lett. **89**, 180402 (2002).

[27] M. Huber, M. Perarnau-Llobet, K. V. Hovhannisyan, P. Skrzypczyk, C. Klöckl, N. Brunner, and A. Acín, Thermodynamic cost of creating correlations, New Journal of Physics **17**, 065008 (2015).

[28] M. Perarnau-Llobet, K. V. Hovhannisyan, M. Huber, P. Skrzypczyk, N. Brunner, and A. Acín, Extractable Work from Correlations, Phys. Rev. X **5**, 041011 (2015).

[29] P. Ćwikliński, M. Studziński, M. Horodecki, and J. Oppenheim, Limitations on the Evolution of Quantum Coherences: Towards Fully Quantum Second Laws of Thermodynamics, Phys. Rev. Lett. **115**, 210403 (2015).

[30] M. Lostaglio, D. Jennings, and T. Rudolph, Description of quantum coherence in thermodynamic processes requires constraints beyond free energy, Nature communications **6**, 6383 (2015).

[31] V. Narasimhachar and G. Gour, Low-temperature thermodynamics with quantum coherence, Nature communications **6**, 7689 (2015).

[32] P. Kammerlander and J. Anders, Coherence and measurement in quantum thermodynamics, Scientific reports **6**, 22174 (2016).

[33] K. Korzekwa, M. Lostaglio, J. Oppenheim, and D. Jennings, The extraction of work from quantum coherence, New Journal of Physics **18**, 023045 (2016).

[34] B. d. L. Bernardo, Unraveling the role of coherence in the first law of quantum thermodynamics, Phys. Rev. E **102**, 062152 (2020).

[35] J. Jaramillo, M. Beau, and A. del Campo, Quantum supremacy of many-particle thermal machines, New Journal of Physics **18**, 075019 (2016).

[36] M. Beau, J. Jaramillo, and A. Del Campo, Scaling-Up Quantum Heat Engines Efficiently via Shortcuts to Adiabaticity, Entropy **18**, 10.3390/e18050168 (2016).

[37] J. Li, T. Fogarty, S. Campbell, X. Chen, and T. Busch, An efficient nonlinear Feshbach engine, New Journal of Physics **20**, 015005 (2018).

[38] Y.-Y. Chen, G. Watanabe, Y.-C. Yu, X.-W. Guan, and A. del Campo, An interaction-driven many-particle quantum heat engine and its universal behavior, npj Quantum Information **5**, 88 (2019).

[39] T. Keller, T. Fogarty, J. Li, and T. Busch, Feshbach engine in the Thomas-Fermi regime, Physical Review Research **2**, 033335 (2020).

[40] M. Boubakour, T. Fogarty, and T. Busch, Interaction-enhanced quantum heat engine, Physical Review Research **5**, 013088 (2023).

[41] J. Koch, K. Menon, E. Cuestas, S. Barbosa, E. Lutz, T. Fogarty, T. Busch, and A. Widera, Making statistics work: a quantum engine in the BEC-BCS crossover, arXiv:2209.14202 (2022).

[42] E. Q. Simmons, R. Sajjad, K. Keithley, H. Mas, J. L. Taxnlimco, E. Nolasco-Martinez, Y. Bai, G. H. Fredrickson, and D. M. Weld, Thermodynamic engine with a quantum degenerate working fluid, arXiv:2304.00659 (2023).

[43] E. H. Lieb and W. Liniger, Exact Analysis of an Interacting Bose Gas. I. The General Solution and the Ground State, Phys. Rev. **130**, 1605 (1963).

[44] C. N. Yang and C. P. Yang, Thermodynamics of a One-Dimensional System of Bosons with Repulsive Delta-Function Interaction, Journal of Mathematical Physics **10**, 1115 (1969).

[45] V. E. Korepin, N. M. Bogoliubov, and A. G. Izergin, *Quantum Inverse Scattering Method and Correlation Functions*, Cambridge Monographs on Mathematical Physics (Cambridge University Press, Cambridge, United Kingdom, 1993).

[46] A. Görlitz, J. M. Vogels, A. E. Leanhardt, C. Raman, T. L. Gustavson, J. R. Abo-Shaeer, A. P. Chikkatur, S. Gupta, S. Inouye, T. Rosenband, and W. Ketterle, Realization of Bose-Einstein Condensates in Lower Dimensions, Phys. Rev. Lett. **87**, 130402 (2001).

[47] M. Greiner, I. Bloch, O. Mandel, T. W. Hänsch, and T. Esslinger, Exploring Phase Coherence in a 2D Lattice of Bose-Einstein Condensates, Phys. Rev. Lett. **87**, 160405 (2001).

[48] F. Schreck, L. Khaykovich, K. L. Corwin, G. Ferrari, T. Bourdel, J. Cubizolles, and C. Salomon, Quasipure Bose-Einstein Condensate Immersed in a Fermi Sea, Phys. Rev. Lett. **87**, 080403 (2001).

[49] M. Greiner, I. Bloch, O. Mandel, T. W. Hänsch, and T. Esslinger, Bose–Einstein condensates in 1D-and 2D optical lattices, Applied Physics B **73**, 769 (2001).

[50] H. Moritz, T. Stöferle, M. Köhl, and T. Esslinger, Exciting Collective Oscillations in a Trapped 1D Gas, Phys. Rev. Lett. **91**, 250402 (2003).

[51] B. L. Tolra, K. M. O'Hara, J. H. Huckans, W. D. Phillips, S. L. Rolston, and J. V. Porto, Observation of Reduced Three-Body Recombination in a Correlated 1D Degenerate Bose Gas, Phys. Rev. Lett. **92**, 190401 (2004).

[52] B. Paredes, A. Widera, V. Murg, O. Mandel, S. Fölling, I. Cirac, G. V. Shlyapnikov, T. W. Hänsch, and I. Bloch, Tonks–Girardeau gas of ultracold atoms in an optical lattice, Nature **429**, 277 (2004).

[53] S. Richard, F. Gerbier, J. H. Thywissen, M. Hugbart, P. Bouyer, and A. Aspect, Momentum Spectroscopy of 1D Phase Fluctuations in Bose-Einstein Condensates,

Phys. Rev. Lett. **91**, 010405 (2003).

[54] T. Stöferle, H. Moritz, C. Schori, M. Köhl, and T. Esslinger, Transition from a Strongly Interacting 1D Superfluid to a Mott Insulator, Phys. Rev. Lett. **92**, 130403 (2004).

[55] T. P. Meyrath, F. Schreck, J. L. Hanssen, C.-S. Chuu, and M. G. Raizen, Bose-Einstein condensate in a box, Phys. Rev. A **71**, 041604 (2005).

[56] T. Kinoshita, T. Wenger, and D. S. Weiss, Observation of a One-Dimensional Tonks-Girardeau Gas, Science **305**, 1125 (2004).

[57] T. Kinoshita, T. Wenger, and D. S. Weiss, Local Pair Correlations in One-Dimensional Bose Gases, Phys. Rev. Lett. **95**, 190406 (2005).

[58] T. Kinoshita, T. Wenger, and D. S. Weiss, A quantum Newton's cradle, Nature **440**, 900 (2006).

[59] J.-B. Trebbia, J. Esteve, C. I. Westbrook, and I. Bouchoule, Experimental Evidence for the Breakdown of a Hartree-Fock Approach in a Weakly Interacting Bose Gas, Phys. Rev. Lett. **97**, 250403 (2006).

[60] J. Esteve, J.-B. Trebbia, T. Schumm, A. Aspect, C. I. Westbrook, and I. Bouchoule, Observations of Density Fluctuations in an Elongated Bose Gas: Ideal Gas and Quasicondensate Regimes, Phys. Rev. Lett. **96**, 130403 (2006).

[61] S. Hofferberth, I. Lesanovsky, B. Fischer, T. Schumm, and J. Schmiedmayer, Non-equilibrium coherence dynamics in one-dimensional Bose gases, Nature **449**, 324 (2007).

[62] A. H. van Amerongen, J. J. P. van Es, P. Wicke, K. V. Kheruntsyan, and N. J. van Druten, Yang-Yang Thermodynamics on an Atom Chip, Phys. Rev. Lett. **100**, 090402 (2008).

[63] P. Krüger, S. Hofferberth, I. E. Mazets, I. Lesanovsky, and J. Schmiedmayer, Weakly interacting bose gas in the one-dimensional limit, Phys. Rev. Lett. **105**, 265302 (2010).

[64] T. Betz, S. Manz, R. Bücker, T. Berrada, C. Koller, G. Kazakov, I. E. Mazets, H.-P. Stimming, A. Perrin, T. Schumm, and J. Schmiedmayer, Two-point phase correlations of a one-dimensional bosonic josephson junction, Phys. Rev. Lett. **106**, 020407 (2011).

[65] J. Armijo, T. Jacqmin, K. V. Kheruntsyan, and I. Bouchoule, Probing Three-Body Correlations in a Quantum Gas Using the Measurement of the Third Moment of Density Fluctuations, Phys. Rev. Lett. **105**, 230402 (2010).

[66] T. Jacqmin, J. Armijo, T. Berrada, K. V. Kheruntsyan, and I. Bouchoule, Sub-Poissonian Fluctuations in a 1D Bose Gas: From the Quantum Quasicondensate to the Strongly Interacting Regime, Phys. Rev. Lett. **106**, 230405 (2011).

[67] J. Armijo, T. Jacqmin, K. Kheruntsyan, and I. Bouchoule, Mapping out the quasicondensate transition through the dimensional crossover from one to three dimensions, Phys. Rev. A **83**, 021605 (2011).

[68] I. Bouchoule, N. J. van Druten, and C. I. Westbrook, Atom chips and one-dimensional Bose gases, in *Atom Chips*, Eds. J. Reichel and V. Vuletic (Wiley-VCH, Weinheim, Germany, 2011).

[69] M. Kuhnert, R. Geiger, T. Langen, M. Gring, B. Rauer, T. Kitagawa, E. Demler, D. Adu Smith, and J. Schmiedmayer, Multimode dynamics and emergence of a characteristic length scale in a one-dimensional quantum system, Phys. Rev. Lett. **110**, 090405 (2013).

[70] B. Yang, Y.-Y. Chen, Y.-G. Zheng, H. Sun, H.-N. Dai, X.-W. Guan, Z.-S. Yuan, and J.-W. Pan, Quantum criticality and the Tomonaga-Luttinger liquid in one-dimensional Bose gases, Phys. Rev. Lett. **119**, 165701 (2017).

[71] S. Erne, R. Bücker, T. Gasenzer, J. Berges, and J. Schmiedmayer, Universal dynamics in an isolated one-dimensional bose gas far from equilibrium, Nature **563**, 225 (2018).

[72] M. Tajik, B. Rauer, T. Schweigler, F. Cataldini, J. ao Sabino, F. S. Møller, S.-C. Ji, I. E. Mazets, and J. Schmiedmayer, Designing arbitrary one-dimensional potentials on an atom chip, Opt. Express **27**, 33474 (2019).

[73] K. V. Kheruntsyan, D. M. Gangardt, P. D. Drummond, and G. V. Shlyapnikov, Pair Correlations in a Finite-Temperature 1D Bose Gas, Phys. Rev. Lett. **91**, 040403 (2003).

[74] K. V. Kheruntsyan, D. M. Gangardt, P. D. Drummond, and G. V. Shlyapnikov, Finite-temperature correlations and density profiles of an inhomogeneous interacting one-dimensional Bose gas, Phys. Rev. A **71**, 053615 (2005).

[75] M. Girardeau, Relationship between Systems of Impenetrable Bosons and Fermions in One Dimension, Journal of Mathematical Physics **1**, 516 (1960).

[76] M. D. Girardeau, Permutation symmetry of many-particle wave functions, Phys. Rev. **139**, B500 (1965).

[77] M. D. Girardeau and E. M. Wright, Breakdown of time-dependent mean-field theory for a one-dimensional condensate of impenetrable bosons, Phys. Rev. Lett. **84**, 5239 (2000).

[78] Y. Castin, R. Dum, E. Mandonnet, A. Minguzzi, and I. Carusotto, Coherence properties of a continuous atom laser, Journal of Modern Optics **47**, 2671 (2000).

[79] C. Mora and Y. Castin, Extension of Bogoliubov theory to quasicondensates, Phys. Rev. A **67**, 053615 (2003).

[80] D. Gangardt and G. Shlyapnikov, Stability and phase coherence of trapped 1D Bose gases, Phys. Rev. Lett. **90**, 010401 (2003).

[81] V. I. Yukalov and M. D. Girardeau, Fermi-Bose mapping for one-dimensional Bose gases, Laser Physics Letters **2**, 375 (2005).

[82] A. Minguzzi and D. M. Gangardt, Exact coherent states of a harmonically confined Tonks-Girardeau gas, Phys. Rev. Lett. **94**, 240404 (2005).

[83] M. Olshanii, Atomic Scattering in the Presence of an External Confinement and a Gas of Impenetrable Bosons, Phys. Rev. Lett. **81**, 938 (1998).

[84] Ultimately, however, the work here is magnetic: it is done by the magnetic field on the atomic dipole moments when $\omega_\perp$ is increased, or vice versa – by the atomic dipole moments on the magnetic field when $\omega_\perp$ is decreased. Alternatively, the change in the interaction strength g can be achieved through control over the scattering length a_s via a magnetic Feshbach resonance [94], in which case the nature of the work is still magnetic.

[85] We use the term Otto cycle in the same sense as used to describe, e.g., a harmonic oscillator Otto engine [20, 37, 38, 41, 95–106], wherein the harmonic oscillator frequency (rather than the volume of the system) is fixed as an external parameter during the thermaliza-

tion strokes. In our case, it is the interaction strength that is fixed, which itself is proportional to the transverse harmonic confinement frequency of the 1D Bose gas; see text.

[86] See the Supplemental Material at http://link.aps.org/supplemental/XXX, which outlines further details on the derivation of the total (integrated) correlation function utilized in the approximate analytic formulation of the net work. Additionally, we present an analysis of the $T_h = T_c$ limit of the harmonically trapped quantum Otto cycle under finite particle flow, along with investigation of engine cycle operation between the asymptotic regimes of the uniform 1D Bose gas [73].

[87] This may be contrasted with the analysis performed in Ref. [38], which was carried out at low energies using the Tomanaga-Luttinger liquid theory for the uniform 1D Bose gas and in the opposite *adiabatic* limit of the sudden quench cycle presented here. ().

[88] C. J. Pethick and H. Smith, *Bose–Einstein condensation in dilute gases* (Cambridge university press, Cambridge, United Kingdom, 2008).

[89] L. Pitaevskii and S. Stringari, *Bose-Einstein condensation and superfluidity*, Vol. 164 (Oxford University Press, Oxford, United Kingdom, 2016).

[90] The cold equilibrium state of Figs. 2 (a) and (b), with linear density ρ, has its interaction strength and temperature parametrized by $\gamma_c = mg_c/\hbar^2\rho$ and $\tau_c = 2mk_BT_c/\hbar^2\rho^2$, respectively.

[91] The cold equilibrium state of Figs. 2 (c) and (d), with $N_c = 2000$ total atoms, has its interaction strength and temperature parameterized as $\overline{g}_c = g_c/l_{\rm ho}\hbar\omega = 0.6$ and $\overline{T}_c = k_BT_c/\hbar\omega = 100$, respectively, where $l_{\rm ho} = \sqrt{\hbar/m\omega}$ is the harmonic oscillator length of the longitudinal harmonic trap of frequency ω. These correspond to dimensionless interaction strength in the trap centre $\gamma_{0,c} = \overline{g}_c/\overline{\rho}_c(0) \simeq 4.9\times10^{-3}$ and temperature $\tau_{0,c} = 2\overline{T}_c/\overline{\rho}_c(0)^2 \simeq 1.3\times10^{-2}$, where $\overline{\rho}_c(0) = \rho_c(0)l_{\rm ho}$ is the dimensionless peak density of the cold thermal equilibrium state.

[92] In practice, this can be realised by establishing diffusive contact between the system and the reservoir, wherein the direction of the net particle flow is controlled by the chemical potential imbalance. Additionally, we note that, as the particle exchange amounts to chemical work, the quantities defined as heat $Q_{\rm in}$ and $Q_{\rm out}$ in the definition of the engine efficiency have to be replaced by the total energy (heat plus chemical work) transferred between the system and reservoirs, $E_{\rm in} = \langle\hat{H}\rangle_{\mathbf{A}} - \langle\hat{H}\rangle_{\mathbf{D}} > 0$ and $E_{\rm out} = \langle\hat{H}\rangle_{\mathbf{B}} - \langle\hat{H}\rangle_{\mathbf{C}} > 0$, respectively. ().

[93] M. Kerr, G. De Rosi, and K. Kheruntsyan, Analytic thermodynamic properties of the Lieb-Liniger gas, to be published (2023).

[94] C. Chin, R. Grimm, P. Julienne, and E. Tiesinga, Feshbach resonances in ultracold gases, Rev. Mod. Phys. **82**, 1225 (2010).

[95] R. Kosloff, A quantum mechanical open system as a model of a heat engine, The Journal of Chemical Physics **80**, 1625 (1984).

[96] H. T. Quan, Y.-x. Liu, C. P. Sun, and F. Nori, Quantum thermodynamic cycles and quantum heat engines, Phys. Rev. E **76**, 031105 (2007).

[97] K. Zhang, F. Bariani, and P. Meystre, Quantum Optomechanical Heat Engine, Phys. Rev. Lett. **112**, 150602 (2014).

[98] Y. Zheng and D. Poletti, Quantum statistics and the performance of engine cycles, Phys. Rev. E **92**, 012110 (2015).

[99] F. Altintas and O. E. Müstecaplıoğlu, General formalism of local thermodynamics with an example: Quantum Otto engine with a spin-1/2 coupled to an arbitrary spin, Phys. Rev. E **92**, 022142 (2015).

[100] R. Kosloff and Y. Rezek, The Quantum Harmonic Otto Cycle, Entropy **19**, 10.3390/e19040136 (2017).

[101] Y. Zheng and D. Poletti, Work and efficiency of quantum Otto cycles in power-law trapping potentials, Phys. Rev. E **90**, 012145 (2014).

[102] G. Watanabe, B. P. Venkatesh, P. Talkner, and A. del Campo, Quantum Performance of Thermal Machines over Many Cycles, Phys. Rev. Lett. **118**, 050601 (2017).

[103] O. Abah and E. Lutz, Energy efficient quantum machines, Europhysics Letters **118**, 40005 (2017).

[104] O. Abah and E. Lutz, Performance of shortcut-to-adiabaticity quantum engines, Phys. Rev. E **98**, 032121 (2018).

[105] G. Watanabe, B. P. Venkatesh, P. Talkner, M.-J. Hwang, and A. del Campo, Quantum Statistical Enhancement of the Collective Performance of Multiple Bosonic Engines, Phys. Rev. Lett. **124**, 210603 (2020).

[106] N. M. Myers, F. J. Peña, O. Negrete, P. Vargas, G. D. Chiara, and S. Deffner, Boosting engine performance with Bose–Einstein condensation, New Journal of Physics **24**, 025001 (2022).

Supplemental Material for: An interaction-driven quantum many-body engine enabled by atom-atom correlations

R. S. Watson, and K. V. Kheruntsyan
School of Mathematics and Physics, University of Queensland, Brisbane, Queensland 4072, Australia
(Dated: August 10, 2023)

We briefly review the Lieb-Liniger model of the one-dimensional (1D) Bose gas with contact interactions in Sec. I, along with the relevant analytic formulas utilized in the main text. In Sec. II we present further results related to Fig. 3 of the main text, elaborating on the limiting case of engine operation under $T_h = T_c$ with finite particle exchange ΔN. In Sec. III we explore sudden quench Otto cycle operation between different (rather than within the same) asymptotic regimes of the 1D Bose gas.

I. THE ONE-DIMENSIONAL BOSE GAS

The uniform 1D Bose gas with repulsive contact interactions is one of a class of integrable models, solvable via the Bethe ansatz, with its ground state first obtained by Lieb and Liniger in 1963 [S1]. This model is described by the second-quantized Hamiltonian

$$\hat{H} = -\frac{\hbar^2}{2m}\int dz \hat{\Psi}^\dagger \frac{\partial^2}{\partial z^2}\hat{\Psi} + \frac{g}{2}\int dz \hat{\Psi}^\dagger\hat{\Psi}^\dagger\hat{\Psi}\hat{\Psi}, \tag{S1}$$

where m is the atomic mass, g is the strength of the contact interactions, and $\hat{\Psi}^\dagger(z)$ and $\hat{\Psi}(z)$ are the bosonic field creation and annihilation operators, respectively. Ground state solutions to this model are dependent only on a single dimensionless interaction strength, $\gamma = mg/\hbar^2\rho$, where $\rho = \langle\hat{\Psi}^\dagger\hat{\Psi}\rangle = N/L$ is the linear density for N particles in a system of size L [S1]. Finite temperature solutions for this model were later discovered by Yang and Yang in 1969 [S2], where they pioneered the thermodynamic Bethe ansatz (TBA), also known as Yang-Yang thermodynamics [S3].

In the early 2000's, rapid development of experimental methods allowed for direct realization of the 1D Bose gas in highly elongated cylindrical traps [S4–S15]. This in turn spurred progress on the theoretical understanding of such systems. A particular focus, due to its experimental relevance [S11, S15], was on calculation of the two-point correlation function [S16–S20], which may be generally defined through

$$g^{(2)}(z,z') = \frac{\langle\hat{\Psi}^\dagger(z)\hat{\Psi}^\dagger(z')\hat{\Psi}(z')\hat{\Psi}(z)\rangle}{\rho(z)\rho(z')}, \tag{S2}$$

where, for a uniform or translationally invariant system (with $\rho(z') = \rho(z) = \rho$), this $g^{(2)}(z,z')$ depends only on the relative distance $|z-z'|$, i.e. $g^{(2)}(z,z') = g^{(2)}(|z-z'|)$. If one is interested in the same point ($z = z'$) correlation function, as utilized in the main text for calculation of the net work and efficiency of the quantum Otto cycle, this in turn becomes $g^{(2)}(0)$.

Based on the analysis of this normalized local (same point) atom-atom correlation function, Kheruntsyan *et al.* found that this model can be characterized by six distinct asymptotic regimes [S18]. These regimes are defined over a parameter space in terms of the dimensionless interaction strength, γ, and a dimensionless temperature, $\tau = 2mk_BT/\hbar^2\rho^2$. Approximate analytic formulas for the $g^{(2)}(0)$ function were obtained in Refs. [S16, S18] in each asymptotic regime, along with numerical means to calculate them via the TBA over the entire parameter space. Further, all analytic thermodynamic quantities, in particular the total energy $\langle\hat{H}\rangle$, were obtained recently for each asymptotic regime in Ref. [S21].

As described in the main text, the local second-order correlation function may be rearranged and integrated for the total correlation function,

$$\begin{aligned}\overline{G^{(2)}} &\equiv \int dz\langle\hat{\Psi}^\dagger(z)\hat{\Psi}^\dagger(z)\hat{\Psi}(z)\hat{\Psi}(z)\rangle \\ &= \int_0^L dz g^{(2)}(0)\rho^2.\end{aligned} \tag{S3}$$

Utilizing the linear density, $\rho = N/L$, this may be expressed as $\overline{G^{(2)}} = N\rho g^{(2)}(0)$, which is utilized in Eq. (3) of the main text for expressing the exact net work of the uniform 1D Bose gas.

In the presence of an external trapping potential, $V(z)$, such as the harmonic confinement considered in the main text, the Hamiltonian given in Eq. (S1) is modified to include an additional term, $\int dz V(z)\hat{\Psi}^\dagger(z)\hat{\Psi}(z)$. Inclusion of such a trapping potential generally breaks the integrability of the system [S22]. However, the solutions derived for a uniform gas may still be utilized within the context of a local density approximation (LDA), which treats the gas as locally uniform, thus remaining amenable to the TBA [S20]. In this approach, both the local correlation function, $g^{(2)}(z,z)$, and the density, $\rho(z)$, are dependent on the position coordinate z.

When calculating the total correlation, $\overline{G^{(2)}}$, for a harmonically trapped system, it was shown in Ref. [S20] that, as the local correlation function is multiplied by the density squared which vanishes rapidly towards the edges of the system, and since the $g^{(2)}(z,z)$ function varies slowly near the trap centre, the function $\overline{G^{(2)}}$ can be well approximated by

$$\overline{G^{(2)}} \simeq g^{(2)}(0,0)\int dz\rho(z)^2, \tag{S4}$$

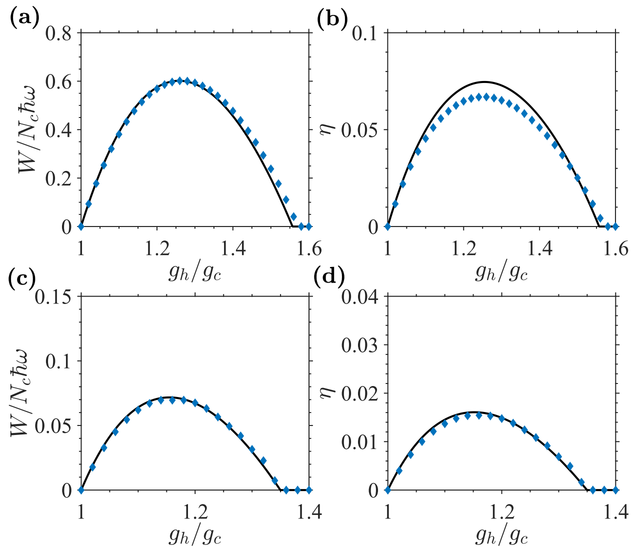

FIG. S1. Analytic and numeric evaluation of chemical engine performance for a harmonically trapped working fluid. Panels (a) and (b) demonstrate performance of the system shown in Fig. 3 of the main text at $T_h = T_c$. The approximate analytic results for net work (solid black line) are seen to agree with their corresponding exact numerical TBA evaluation (blue diamonds). In panels (c) and (d), we show the performance of a chemical engine within the strongly interacting (near Tonks-Girardeau) regime ($\gamma_0 \gg 1$, $\tau_0 \ll 1$) [S20, S21] under a particle transfer of $\Delta N = 5$, and with $N_c = 20$. The cold thermal equilibrium state is defined by a dimensionless interaction strength $\overline{g}_c = 20$, and temperature $\overline{T}_c = \overline{T}_h = 1$, corresponding to $\gamma_{0,c} = 8.56$ and $\tau_{0,c} = 0.37$.

where $g^{(2)}(0,0)$ is the local atom-atom correlation function at the trap centre, $z = 0$. Further, as introduced in the main text, the integral over the squared density may parametrized via $\int dz\rho(z)^2 = bN\rho(0)$, where

$$b = \frac{\int dz\rho(z)^2}{N\rho(0)}. \tag{S5}$$

The numerical value of this constant can be evaluated numerically using the TBA, or approximated analytically using, e.g., the Thomas-Fermi density profile (see Appendix A of the main text). We note here that, in all asymptotic regimes where an analytic density profile of the 1D Bose gas may be formulated, the b parameter may be expressed as a constant of order one. Through this, we arrive at an approximate form for the total correlation function in a harmonic trap, $\overline{G^{(2)}} \simeq Nb\rho(0)g^{(2)}(0,0)$, which is utilized in the approximate expression for net work given in Eq. (4) of the main text.

II. CHEMICAL ENGINE PERFORMANCE

For a quantum Otto cycle utilizing diffusive system-reservoir contact, one may consider the case of a purely chemical engine [S23, S24], where there is no net heat flow between the system and reservoirs over the time that they are in contact, therefore corresponding to $T_h = T_c$. Such a chemical engine may be realized within the context of the harmonically trapped 1D Bose gas described in Eq. (4) of the main text, achieving positive net work via the linear scaling with N_h and N_c (see also Ref. [82] of the main text).

Net work and efficiency of a chemical engine for a harmonically trapped 1D Bose gas in the weakly interacting quasicondensate regime [S20, S21] ($\gamma_0 \ll \tau_0 \ll \sqrt{\gamma_0}$) are demonstrated in Fig. S1 (a) and (b), respectively, and represent the $T_h/T_c = 1$ limit of Fig. 3 in the main text. Here, we see excellent agreement between the approximate analytic results, shown as solid black lines, and the exact TBA numerics, shown as blue diamonds. Positivity of the net work shown Fig. S1 (a) over a certain range of the ratio of interaction strengths stems from the enhancement of net work under a finite particle exchange (i.e. $N_h \neq N_c$ in Eq.(4) of the main text). The eventual turnover and approach to zero net work emerges due to the scaling of the peak density of the Thomas-Fermi parabola for the hot thermal state, $\overline{\rho}_h(0) \propto 1/\overline{g}_h^{1/3}$ (see Appendix A of the main text), which inevitably reduces the net work to zero for a large enough quench.

Similarly to Figs. S1 (a) and (b), chemical engine performance for a harmonically trapped gas, but in the strongly interacting near Tonks-Girardeau regime [S20, S21] ($\gamma_0 \gg 1$, $\tau_0 \ll 1$) is demonstrated in Figs. S1 (c) and (d), for $N_c = 20$ particles, and $\Delta N = 5$. The net work for this engine cycle is nearly an order of magnitude lower than that for the weakly interacting gas due to its dependence on the peak density, $\overline{\rho}(0) \simeq \sqrt{2N/\pi^2}$ [S20], which is independent of both temperature and interaction strength, and is an order of magnitude smaller than the peak density of the weakly interacting gas due to the lower atom number of the working fluid that we consider in this regime. (The lower total atom number considered is consistent with typically low atom numbers that used in experimental realizations of the Tonks-Girardeau regime [S10, S15, S25]).

Positivity of net work for the strongly interacting gas at $T_h = T_c$, as for the weakly interacting gas, is enabled by the finite particle exchange. However, as the peak density is independent of interaction strength, the eventual turnover and convergence to zero net work stems instead from the dependence of the net work on the local second order correlation function, which can be approximated as [S20, S21]:

$$g^{(2)}(0,0) \simeq \frac{4}{3}\left(\frac{\pi}{\gamma_0}\right)^2\left[1 + \frac{\tau_0^2}{4\pi^2}\right], \ (\gamma_0 \gg 1, \tau_0 \ll 1). \tag{S6}$$

Here, the scaling with interaction strength as $g_h^{(2)} \propto 1/\overline{g}^2$ reduces the net work to zero for a smaller ratio of interaction strength than observed in the weakly interacting case. We again observe that the approximate analytic evaluation of both net work and efficiency of the cycle is in excellent agreement with the exact TBA numerics.

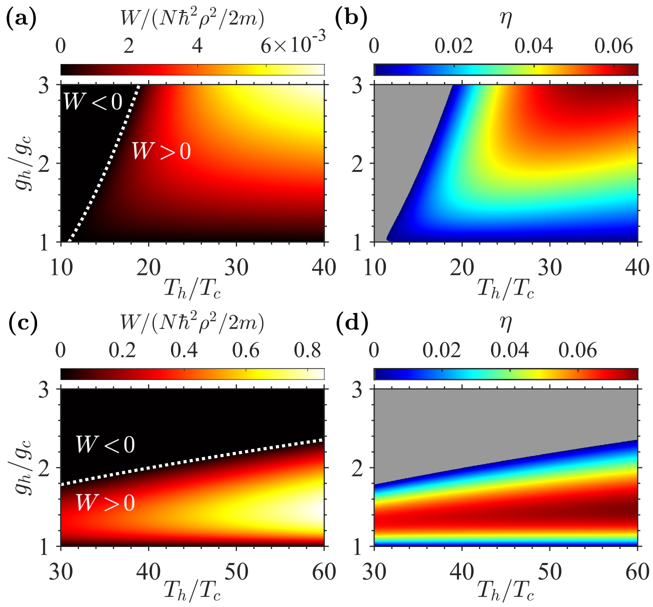

FIG. S2. Inter-regime operation of the interaction-driven quantum Otto cycle with a uniform 1D Bose gas as a working fluid. Panels (a) and (b) demonstrate operation of the Otto cycle with a weakly interacting working fluid. Here, the cold thermal equilibrium state is the same as in Figs. 2 (a) and (b) of the main text, and the hot thermal equilibrium states are in the decoherent quantum regime ($\sqrt{\gamma} \ll \tau \ll 1$) [S18]. In panels (c) and (d) we show an engine cycle with a strongly interacting working fluid. For this cycle, the cold thermal equilibrium state is in the strongly interacting (near Tonks-Girardeau) regime ($\gamma \gg 1$, $\tau \ll 1$), with a dimensionless interaction strength $\gamma_c = 8.56$, and temperature $\tau_c = 0.37$. The hot thermal equilibrium states of this cycle lie within the asymptotic regime of high-temperature fermionization ($1 \ll \tau \ll \gamma^2$) [S18].

III. INTER-REGIME OPERATION WITH A UNIFORM WORKING FLUID

Thus far, investigation of the sudden quench quantum Otto cycle has been restricted to operation entirely within a single asymptotic regime. However, thanks to the generality of the formulas for net work and efficiency, we may additionally consider the possibility of investigating operation *between* these regimes. Transitioning between the various asymptotic regimes typically requires a large quench of interaction strength, a large temperature difference, or a combination of the two. This makes operation between non-adjacent regimes physically unfeasible for realization in the laboratory. Additionally, we note that, at low temperatures, the local second-order correlation function in the quasicondensate regime (taken to be at g_c) is given by $g^{(2)}(0) \simeq 1$ to lowest order, whereas in the strongly interacting Tonks-Girardeau regime (taken to be at g_h), it is reduced to $g^{(2)}(0) \simeq 0$. This results in no positive net work for a uniform system under a large ratio of interaction strength, according to the analysis presented in the main text. For this reason, we consider only inter-regime operations with a large temperature ratio in conjunction with an interaction strength ratio of order one.

Inter-regime operation of the sudden quench Otto cycle is explored in Fig. S2 for a uniform working fluid. Panels (a) and (b) demonstrate performance for a cycle with a cold thermal equilibrium state **C** with the same parameters as that in Fig. 2(a) and (b) of the main text. Hot thermal equilibrium states **A**, on the other hand, are chosen such that they lie within the adjacent decoherent quantum regime ($\sqrt{\gamma} \ll \tau \ll 1$), where $g^{(2)}(0) \simeq 2 - 4\gamma/\tau^2$ [S18]. For both net work and efficiency, we observe a similar structure when comparing with that of the cycle lying entirely within a single regime, shown in Fig. 2(a) and (b) in the main text, with this inter-regime cycle generating greater net work due to the increased temperature ratio for inter-regime operation.

Performance of an inter-regime engine cycle with a strongly interacting uniform working fluid is shown in Fig. S2 (c) and (d), where the cold thermal equilibrium state lies in the Tonks-Girardeau regime, and the hot thermal equilibrium states are chosen to fall within the neighboring regime of high-temperature fermionization ($1 \ll \tau \ll \gamma^2$), where $g^{(2)}(0) \simeq 2\tau/\gamma^2$ [S18]. We see that, for a similar ratio of both interaction strength and temperature, inter-regime engine operation with a strongly interacting working fluid produces larger net work than that observed in the weakly interacting regime at the cost of a reduction of parameter space over which positive net work is possible. This suggests that, in contrast to the operation of an engine cycle that remains entirely within a single asymptotic regime, if one can afford pursuing an engine cycle operating under a large temperature difference, a strongly interacting gas may be capable of a greater net work than a weakly interacting one with the same efficiency.

[S1] E. H. Lieb and W. Liniger, Exact Analysis of an Interacting Bose Gas. I. The General Solution and the Ground State, Phys. Rev. **130**, 1605 (1963).

[S2] C. N. Yang and C. P. Yang, Thermodynamics of a One-Dimensional System of Bosons with Repulsive Delta-Function Interaction, Journal of Mathematical Physics **10**, 1115 (1969).

[S3] A. H. van Amerongen, J. J. P. van Es, P. Wicke, K. V. Kheruntsyan, and N. J. van Druten, Yang-Yang Thermodynamics on an Atom Chip, Phys. Rev. Lett. **100**, 090402 (2008).

[S4] M. Greiner, I. Bloch, O. Mandel, T. W. Hänsch, and T. Esslinger, Exploring Phase Coherence in a 2D Lattice of Bose-Einstein Condensates, Phys. Rev. Lett. **87**, 160405 (2001).

[S5] A. Görlitz, J. M. Vogels, A. E. Leanhardt, C. Raman,

T. L. Gustavson, J. R. Abo-Shaeer, A. P. Chikkatur, S. Gupta, S. Inouye, T. Rosenband, and W. Ketterle, Realization of Bose-Einstein Condensates in Lower Dimensions, Phys. Rev. Lett. **87**, 130402 (2001).

[S6] F. Schreck, L. Khaykovich, K. L. Corwin, G. Ferrari, T. Bourdel, J. Cubizolles, and C. Salomon, Quasipure Bose-Einstein Condensate Immersed in a Fermi Sea, Phys. Rev. Lett. **87**, 080403 (2001).

[S7] M. Greiner, I. Bloch, O. Mandel, T. W. Hänsch, and T. Esslinger, Bose–Einstein condensates in 1D-and 2D optical lattices, Applied Physics B **73**, 769 (2001).

[S8] S. Richard, F. Gerbier, J. H. Thywissen, M. Hugbart, P. Bouyer, and A. Aspect, Momentum Spectroscopy of 1D Phase Fluctuations in Bose-Einstein Condensates, Phys. Rev. Lett. **91**, 010405 (2003).

[S9] H. Moritz, T. Stöferle, M. Köhl, and T. Esslinger, Exciting Collective Oscillations in a Trapped 1D Gas, Phys. Rev. Lett. **91**, 250402 (2003).

[S10] T. Kinoshita, T. Wenger, and D. S. Weiss, Observation of a One-Dimensional Tonks-Girardeau Gas, Science **305**, 1125 (2004).

[S11] B. L. Tolra, K. M. O'Hara, J. H. Huckans, W. D. Phillips, S. L. Rolston, and J. V. Porto, Observation of Reduced Three-Body Recombination in a Correlated 1D Degenerate Bose Gas, Phys. Rev. Lett. **92**, 190401 (2004).

[S12] B. Paredes, A. Widera, V. Murg, O. Mandel, S. Fölling, I. Cirac, G. V. Shlyapnikov, T. W. Hänsch, and I. Bloch, Tonks–Girardeau gas of ultracold atoms in an optical lattice, Nature **429**, 277 (2004).

[S13] T. Stöferle, H. Moritz, C. Schori, M. Köhl, and T. Esslinger, Transition from a Strongly Interacting 1D Superfluid to a Mott Insulator, Phys. Rev. Lett. **92**, 130403 (2004).

[S14] T. P. Meyrath, F. Schreck, J. L. Hanssen, C.-S. Chuu, and M. G. Raizen, Bose-Einstein condensate in a box, Phys. Rev. A **71**, 041604 (2005).

[S15] T. Kinoshita, T. Wenger, and D. S. Weiss, Local Pair Correlations in One-Dimensional Bose Gases, Phys. Rev. Lett. **95**, 190406 (2005).

[S16] D. Gangardt and G. Shlyapnikov, Local correlations in a strongly interacting one-dimensional Bose gas, New Journal of Physics **5**, 79 (2003).

[S17] D. Gangardt and G. Shlyapnikov, Stability and phase coherence of trapped 1D Bose gases, Phys. Rev. Lett. **90**, 010401 (2003).

[S18] K. V. Kheruntsyan, D. M. Gangardt, P. D. Drummond, and G. V. Shlyapnikov, Pair Correlations in a Finite-Temperature 1D Bose Gas, Phys. Rev. Lett. **91**, 040403 (2003).

[S19] P. D. Drummond, P. Deuar, and K. V. Kheruntsyan, Canonical Bose Gas Simulations with Stochastic Gauges, Phys. Rev. Lett. **92**, 040405 (2004).

[S20] K. V. Kheruntsyan, D. M. Gangardt, P. D. Drummond, and G. V. Shlyapnikov, Finite-temperature correlations and density profiles of an inhomogeneous interacting one-dimensional Bose gas, Phys. Rev. A **71**, 053615 (2005).

[S21] M. Kerr, G. De Rosi, and K. Kheruntsyan, Analytic thermodynamic properties of the Lieb-Liniger gas, to be published (2023).

[S22] I. E. Mazets, Integrability breakdown in longitudinaly trapped, one-dimensional bosonic gases, The European Physical Journal D **65**, 43 (2011).

[S23] L. Chen, F. Sun, C. Wu, and J. Yu, Performance characteristic of isothermal chemical engines, Energy Conversion and Management **38**, 1841 (1997).

[S24] H. Hooyberghs, B. Cleuren, A. Salazar, J. O. Indekeu, and C. Van den Broeck, Efficiency at maximum power of a chemical engine, The Journal of Chemical Physics **139**, 134111 (2013).

[S25] T. Kinoshita, T. Wenger, and D. S. Weiss, A quantum Newton's cradle, Nature **440**, 900 (2006).